Single-Spin Readout and Quantum Sensing Using Optomechanically Induced Transparency

Martin Koppenhöfer, Carl Padgett, Jeffrey V. Cady, Viraj Dharod, Hyunseok Oh, Ania C. Bleszynski Jayich, and A. A. Clerk

Single-Spin Readout and Quantum Sensing using Optomechanically-Induced Transparency

Martin Koppenhöfer[1], Carl Padgett[2], Jeffrey V. Cady[2],

Viraj Dharod[2], Hyunseok Oh[2], Ania C. Bleszynski Jayich[2], and A. A. Clerk[1]

[1]*Pritzker School of Molecular Engineering, University of Chicago, Chicago, IL 60637, USA*

[2]*Department of Physics, University of California Santa Barbara, Santa Barbara, CA 93106, USA*

(Dated: January 31, 2023)

Solid-state spin defects are promising quantum sensors for a large variety of sensing targets. Some of these defects couple appreciably to strain in the host material. We propose to use this strain coupling for mechanically-mediated dispersive single-shot spin readout by an optomechanically-induced transparency measurement. Surprisingly, the estimated measurement times for negatively-charged silicon-vacancy defects in diamond are an order of magnitude shorter than those for single-shot optical fluorescence readout. Our scheme can also be used for general parameter-estimation metrology and offers a higher sensitivity than conventional schemes using continuous position detection.

Introduction— Solid-state defect spins are promising candidates to build powerful quantum sensors [1–4] as well as memories and repeaters for quantum communication [5]. They have a small footprint [6, 7], straightforward operation, and are susceptible to a large variety of sensing targets, such as magnetic [8, 9] and electric fields [10] as well as temperature [11]. Quantum applications (e.g., entanglement-assisted metrology [12–14]) require high-fidelity single-shot spin readout. Optical spin readout is desirable but, unfortunately, not provided by all types of spin defects. Moreover, even many optically addressable spin defects fail to reach robust high-fidelity single-shot readout [5, 15], e.g., because of low photon collection efficiencies, inconvenient optical frequencies, or limited readout times due to non-spin-conserving transitions between orbital ground and excited states.

These issues motivate asking whether other interactions could be harnessed for readout. Recently, it has been shown that some spin defects have an appreciable coupling to strain arising from mechanical vibrations in their host material [16–18]. It has been suggested to use this strain coupling for mechanical cooling [19], mechanical control of the spin defect [16, 20–24], and reservoir engineering [25, 26]. The mechanical mode can also be strongly coupled to electromagnetic modes, e.g., by shaping the host material into an optomechanical crystal (OMC) [27], which enables optical control and fiber-coupled telecom-wavelength optical access, instead of more challenging free-space optical access that is often in the visible range. Diamond OMCs with large optomechanical coupling and integrated nitrogen-vacancy (NV) defects have already been demonstrated experimentally [24, 28, 29].

In this Letter, we show that strain coupling can be used for another crucial functionality: it can enable rapid all-optical dispersive readout of a single solid-state spin, without any orbital excitation. Dispersive readout enables fast, high-fidelity, and quantum-nondemolition (QND) detection in a variety of platforms, including superconducting qubits [30], where the state of the qubit
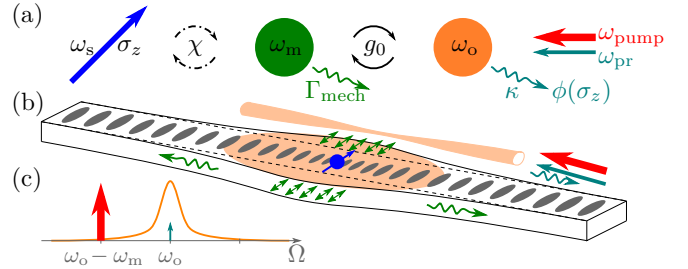

FIG. 1. Dispersive spin readout using optomechanically-induced transparency (OMIT). (a) Sketch of the considered hybrid optomechanical system. A mechanical mode (green circle, center) interacts both with a single spin (blue arrow, left) via a strain-coupling-mediated dispersive interaction, and with an optical mode (orange circle, right) via optomechanical interaction. The optical mode is driven by a pump and a probe laser implementing an OMIT scheme. The σ_z projection of the spin state is encoded in the phase $\phi(\sigma_z)$ of the reflected probe light. All other parameters are defined in the main text. (b) Sketch of a possible experimental implementation using a diamond optomechanical crystal (OMC) with an embedded spin defect (blue) strain-coupled to a mechanical breathing mode (green straight arrows). The optical mode (orange) of the OMC is evanescently coupled to a tapered fiber for optical driving and homodyne detection. (c) Frequencies of the pump and probe lasers. The solid orange curve is the Lorentzian cavity response with width $\kappa < \omega_{\mathrm{m}}$.

shifts the resonance frequency of a driven microwave cavity and is encoded in the phase of the microwave output field. Using strain coupling, one could try to replicate this by replacing the microwave cavity with a driven, dispersively-coupled mechanical mode. Qubit readout would then require an effective homodyne detection of emitted phonons, which could be done optically using mechanics-to-optics transduction. The scheme we introduce mimics this kind of measurement in a simple and resource-efficient fashion, by exploiting one of the most ubiquitous effects in optomechanics: optomechanically-induced transparency (OMIT) [31–34], where a mechanical mode alters the density-of-states of an optical cavity.

While OMIT has been used extensively for device calibration, we show here that, surprisingly, it also paves a powerful route to all-optical single-shot solid-state spin readout (no explicit mechanical driving or readout is needed). Note that our OMIT-based scheme is distinct from the recently demonstrated optical readout of a superconducting qubit using optomechanical microwave-to-optical transduction [35, 36].

As a promising experimental example, we analyze readout of a silicon-vacancy (SiV) defect coupled to a diamond OMC. Surprisingly, the estimated spin readout times for realistic experimental parameters [28, 29, 37, 38] are more than a factor of four shorter than the ones for optical cavity-based SiV readout [39], and an order of magnitude shorter than the best optical fluorescence readout times for SiV centers [40] (which are limited by the repolarization timescale of the spin defect into its ground state and require precise alignment of the magnetic field along the SiV axis). In contrast, our dispersive readout is in principle a QND measurement. We stress that our protocol can be applied to other spin-defects (beyond SiV centers) with sufficiently large strain coupling but potentially no optical addressability, since we only assume coupling of an effective two-level system to a mechanical mode.

We also demonstrate that our OMIT-based sensing protocol has applications beyond qubit readout: it can be used for parameter sensing in any optomechanical system where the mechanical frequency depends on an unknown parameter. It exceeds fundamental sensitivity limits that constrain standard schemes employing continuous mechanical position detection [e.g., as used in atomic-force-microscopy (AFM) [41, 42] and mass sensing [43]].

The system— We consider a standard optomechanical (OM) system, sketched in Figs. 1(a,b), with Hamiltonian $\hat{H}_{\mathrm{om}} = \omega_{\mathrm{o}}\hat{a}^\dagger\hat{a} + \omega_{\mathrm{m}}\hat{b}^\dagger\hat{b} - g_0\hat{a}^\dagger\hat{a}(\hat{b} + \hat{b}^\dagger)$. Here, $\hat{a}$ ($\hat{b}$) is the annihilation operator of the optical (mechanical) mode with frequency ω_{o} (ω_{m}), g_0 is the bare OM coupling strength, and $\hbar = 1$. Both modes interact with dissipative Markovian environments which lead to a decay of optical (mechanical) excitations at a rate κ (Γ_{mech}), with $\kappa \gg \Gamma_{\mathrm{mech}}$. For simplicity, we envisage a several-GHz mechanical mode in a dilution refrigerator, such that thermal occupation is negligible [44].

The mechanical mode is dispersively coupled to a spin, $\hat{H}_{\mathrm{sm}} = \omega_{\mathrm{s}}\hat{\sigma}_z/2 - \chi\hat{\sigma}_z\hat{b}^\dagger\hat{b}$, where $\hat{\sigma}_z$ is the Pauli z matrix (and commutes with the spin-only Hamiltonian), ω_{s} is the splitting between the two energy levels, and χ is the dispersive coupling strength. Depending on the σ_z projection of the spin state, the mechanical frequency is shifted by $\varepsilon = -\sigma_z\chi$. In principle, the mechanical frequency shift ε can be measured by driving the mechanical mode with a linear drive and by measuring the phase of the phonons emitted from the mechanical mode into

the substrate; this would be a mechanical analogue of a standard cavity QED dispersive readout [30]. Of course, directly measuring these emitted phonons is infeasible in most setups.

To overcome this issue, we propose an OMIT measurement [31–34], which employs two laser drives as shown in Fig. 1(c). The strong red-detuned pump laser, $\omega_{\mathrm{pump}} = \omega_{\mathrm{o}} - \omega_{\mathrm{m}}$, causes additional mechanical damping and converts part of the dissipated phonons into an optical output field, thus rendering them accessible to conventional optical homodyne detection. Via the OM interaction, it also converts the weak optical probe laser into a linear mechanical drive. Together, these enable all-optical readout of ε, as we now show.

Consider first the situation with only the strong pump laser. It allows us to separate the cavity field into a semiclassical amplitude $a \gg 1$ and quantum fluctuations $\hat{d}$ around it, $\hat{a} = e^{-i\omega_{\mathrm{pump}}t}(a + \hat{d})$. Similarly, we decompose the mechanical mode $\hat{b} = b + \hat{c}$ and linearize the OM interaction [45]. We further assume the good cavity limit $\omega_{\mathrm{m}} \gg \kappa$, allowing us to make a rotating wave approximation on the OM interaction. In a frame rotating at ω_{pump}, the approximate linearized Hamiltonian is:

$$\hat{H} \approx \omega_{\mathrm{m}}\hat{d}^\dagger\hat{d} + (\omega_{\mathrm{m}} + \varepsilon)\hat{c}^\dagger\hat{c} - G\left(\hat{c}^\dagger\hat{d} + \hat{d}^\dagger\hat{c}\right) , \quad (1)$$

where $G = g_0a$ is the optically-enhanced coupling strength. At time $t = 0$ the weak probe laser at frequency ω_{pr} is switched on. We account for this through the cavity input field, $\hat{d}_{\mathrm{in}}(t \geq 0) = a_{\mathrm{pr,in}}e^{-i\omega_{\mathrm{m}}t} + \hat{\xi}_{\mathrm{in}}(t)$, where $\hat{\xi}_{\mathrm{in}}(t)$ is input vacuum noise and $|a_{\mathrm{pr,in}}|^2$ is the photon flux of the probe laser. Note that $\hat{d}_{\mathrm{in}}$ describes a probe laser which is resonant with the optical cavity in the lab frame, cf. Fig. 1(c). We also considered a detuned probe laser but found the resonant case to be optimal for qubit readout [38].

Signal-to-noise ratio (SNR)— For $a_{\mathrm{pr,in}} \geq 0$ and $\kappa \gg \Gamma_{\mathrm{mech}}$, the mechanical frequency shift ε is encoded in the $\varphi = \pi/2$ quadrature of the optical output field $\hat{d}_{\mathrm{out}}(t) = \sqrt{\kappa}\hat{d}(t) + \hat{d}_{\mathrm{in}}(t)$ and can be measured by optical homodyne detection. Using the measurement operator describing the integrated homodyne current from $t = 0$ to $t = \tau$,

$$\hat{\mathcal{I}}(\tau) = \sqrt{\kappa}\int_0^\tau \mathrm{d}t\,\left[e^{i\varphi}e^{-i\omega_{\mathrm{m}}t}\hat{d}_{\mathrm{out}}^\dagger(t) + \mathrm{h.c.}\right] , \quad (2)$$

the SNR at time τ of our qubit σ_z measurement is defined as [46]

$$\mathrm{SNR}^2(\tau) = \frac{|\langle\hat{\mathcal{I}}(\tau)\rangle_{-\chi} - \langle\hat{\mathcal{I}}(\tau)\rangle_{+\chi}|^2}{\langle[\widehat{\delta\mathcal{I}}(\tau)]^2\rangle_{-\chi} + \langle[\widehat{\delta\mathcal{I}}(\tau)]^2\rangle_{+\chi}} , \quad (3)$$

where $\widehat{\delta\mathcal{I}}(\tau) = \hat{\mathcal{I}}(t) - \langle\hat{\mathcal{I}}(\tau)\rangle_\varepsilon$ and $\langle\cdot\rangle_\varepsilon$ denotes an expectation value with the mechanical resonance frequency shifted by ε. We focus on the usual limit $G \ll \kappa$ where there is no many-photon OM strong coupling, and
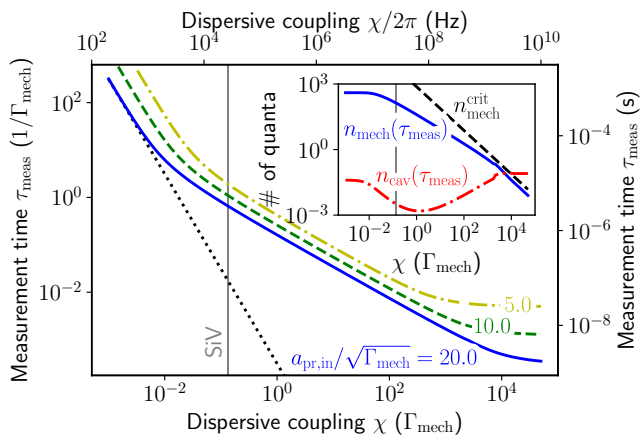
FIG. 2. Minimum measurement time τ_{meas} required to reach a signal-to-noise ratio (SNR) of unity as a function of the spin-mechanical dispersive coupling strength χ. The optomechanical cooperativity C_{om} has been optimized for each data point. The dotted black line indicates the asymptotic form of the measurement time for $\chi/\Gamma_{\mathrm{mech}} \ll 1$ [Eq. (5)]. It is off by almost two orders of magnitude for the expected parameters for SiV defects in a diamond OMC (gray vertical line). Inset: Phonon number $n_{\mathrm{mech}}(\tau_{\mathrm{meas}})$, photon number $n_{\mathrm{cav}}(\tau_{\mathrm{meas}})$, and critical phonon number $n_{\mathrm{mech}}^{\mathrm{crit}}$ for $a_{\mathrm{pr,in}}/\sqrt{\Gamma_{\mathrm{mech}}} = 20.0$, g_{sm} varied, $\Delta_{\mathrm{sm}}/\Gamma_{\mathrm{mech}} = 750$, and $\kappa/\Gamma_{\mathrm{mech}} = 10000$.

where $\chi \ll \kappa$. Note that the effects of χ can still be non-perturbative if $\chi \gtrsim \Gamma_{\mathrm{mech}}$. Using the Heisenberg-Langevin equations for our system [38], we find

$$\mathrm{SNR}^2(\tau) = 8\,|a_{\mathrm{pr,in}}|^2 \left(\frac{C_{\mathrm{om}}}{1+C_{\mathrm{om}}}\right)^2 \sin^2(2\xi)\,\tau\,[1-F(\tau)]^2 \;,$$

(4)

where $F(\tau) = \frac{1}{\chi\tau}[\sin(2\xi) - \sin(2\xi + \chi\tau)e^{-\Gamma_{\mathrm{mech}}(1+C_{\mathrm{om}})\tau/2}]$. The OM cooperativity $C_{\mathrm{om}} = 4G^2/\kappa\Gamma_{\mathrm{mech}}$ can be tuned by varying the pump laser amplitude. As in standard dispersive readout, depending on the frequency shift $\varepsilon = \pm\chi$, $\hat{d}_{\mathrm{out}}(t)$ evolves into one of two different coherent states separated by an angle $2\xi = 2\arctan[2\chi/\Gamma_{\mathrm{mech}}(1 + C_{\mathrm{om}})]$. Equation (4) maps to a standard cQED dispersive readout where the cavity damping rate has been replaced by an optically-tunable mechanical damping rate $\Gamma_{\mathrm{mech}}(1+C_{\mathrm{om}})$, and where only a fraction $C_{\mathrm{om}}/(1+C_{\mathrm{om}})$ of the total output flux is detected. As we show, this additional tunability leads to important differences in readout optimization and dynamics.

Measurement time— The measurement time is implicitly defined by $\mathrm{SNR}^2(\tau_{\mathrm{meas}}) = 1$, and our goal is to optimize C_{om} such that τ_{meas} is minimal. As shown in Fig. 2, there are three scalings of τ_{meas} with χ: (i) For a weak strain coupling $\chi \ll \Gamma_{\mathrm{mech}}, \kappa$, the intrinsic mechanical ringup time $1/\Gamma_{\mathrm{mech}}$ will be much shorter than τ_{meas}. The measurement is fastest if the impedance-matching

condition $C_{\mathrm{om}} = 1$ holds, in which case

$$\tau_{\mathrm{meas}} \to \frac{\Gamma_{\mathrm{mech}}^2}{8\,|a_{\mathrm{pr,in}}|^2\,\chi^2} \;.$$

(5)

In this regime, the probe laser leads to a steady-state mechanical phonon number $n_{\mathrm{mech}}^{\mathrm{ss}} = \lim_{\tau\to\infty} n_{\mathrm{mech}}(\tau) = |a_{\mathrm{pr,in}}|^2/\Gamma_{\mathrm{mech}}$ on a timescale shorter than τ_{meas}. (ii) As we show below, spin defects can reach appreciable strain coupling $\chi \gtrsim \Gamma_{\mathrm{mech}}$ such that $\mathrm{SNR}^2(\tau) = 1$ is achieved before the mechanical steady state is reached. In this regime, is it advantageous to increase C_{om} beyond 1 to speed up the mechanical ring-up, so that this occurs on the same timescale as the measurement (i.e., $C_{\mathrm{om}} \propto 1/\Gamma_{\mathrm{mech}}\tau_{\mathrm{meas}}$). For an optimal C_{om}, we find in this regime $\tau_{\mathrm{meas}} \propto (\chi\,|a_{\mathrm{pr,in}}|)^{-2/3}$. (iii) Finally, for $\chi \gg \Gamma_{\mathrm{mech}}$, the large detuning $\pm\chi$ between the mechanical mode and the probe laser becomes the limiting factor of the measurement. The optimal cooperativity $C_{\mathrm{om}} = 2\chi/\Gamma_{\mathrm{mech}}$ strongly broadens the mechanical linewidth such that transient dynamics becomes irrelevant again and the measurement time converges to a constant value which depends only on the rate at which probe photons are sent into the system,

$$\tau_{\mathrm{meas}} \to \frac{1}{8\,|a_{\mathrm{pr,in}}|^2} \;.$$

(6)

Note that OMIT allows one to optimize the effective damping rate for different values of the dispersive coupling such that one can take advantage of large couplings $\chi \gg \Gamma_{\mathrm{mech}}$.

Critical phonon number— Figure 2 reveals several interesting features. First, τ_{meas} can be smaller than $1/\Gamma_{\mathrm{mech}}$, which reflects the fact that we can broaden the mechanical linewidth optically, $\Gamma_{\mathrm{mech}}(1 + C_{\mathrm{om}}) \gg \Gamma_{\mathrm{mech}}$. Second, τ_{meas} is short because we are using many probe phonons. As shown in the inset of Fig. 2, this does not come at the cost of a high photon number (which could cause unwanted heating) since $n_{\mathrm{mech}}^{\mathrm{ss}}/n_{\mathrm{cav}}^{\mathrm{ss}} = \Gamma_{\mathrm{mech}}\kappa C_{\mathrm{om}}/(\Gamma_{\mathrm{mech}}^2 + 4\varepsilon^2) \propto \kappa/\Gamma_{\mathrm{mech}} \gg 1$. Further, with increasing $\chi/\Gamma_{\mathrm{mech}}$, the optimized C_{om} grows and $n_{\mathrm{mech}}^{\mathrm{ss}}$ decreases (as the total mechanical damping is $\propto C_{\mathrm{om}}$). Corrections to the dispersive spin-mechanical interaction define a critical phonon number $n_{\mathrm{mech}}^{\mathrm{crit}}$ (see [38]), which limits the maximum probe power, determines the plateau value of τ_{meas} for $\chi \gg \Gamma_{\mathrm{mech}}$, and prevents infinitely fast measurements [47].

Feasibility criteria— For QND readout, one needs $\tau_{\mathrm{meas}} \ll \min(T_1, \tau_{\mathrm{Purcell}})$, where $T_1 = 2\pi/\gamma_{\mathrm{rel}}$ is the single-spin relaxation time and τ_{Purcell} the Purcell decay time. As we show below, this is well within reach for a single SiV defect coupled to a diamond OMC. For other defects with smaller strain coupling, this condition can still be achieved in an ensemble of N spins. In the regime $\chi \ll \Gamma_{\mathrm{mech}}$, one then obtains the conditions $\Delta_{\mathrm{sm}}/\Gamma_{\mathrm{mech}} \gg \sqrt{N/8}$ (to suppress collective Purcell decay) and $4Ng_{\mathrm{sm}}^2/\Gamma_{\mathrm{mech}}\gamma_{\mathrm{rel}} \gg 1/2$ [38].

Application to SiV systems— As a concrete example, we show that readout a single SiV defect embedded in a state-of-the-art diamond OMC is experimentally feasible. Diamond OMCs with $\kappa/2\pi \approx 2\,\mathrm{GHz}$ have recently been demonstrated by Burek *et al.* [28] and Cady *et al.* [29]. The mechanical modes had $\omega_\mathrm{m}/2\pi \approx 6\,\mathrm{GHz}$ and quality factors up to 4100 at room temperature with higher values expected at cryogenic temperatures [28]. A mechanical damping rate $\Gamma_\mathrm{mech}/2\pi = 200\,\mathrm{kHz}$ seems thus feasible. The measured optomechanical couplings are $g_0/2\pi \approx 200\,\mathrm{kHz}$ [28, 29]. Spin-mechanical single phonon coupling rates for SiV defects in an OMC have been estimated to be $g_\mathrm{sm}/2\pi \approx 2\,\mathrm{MHz}$ [37]. Surprisingly, the strain coupling can be tuned up to $g_\mathrm{sm}/2\pi \approx 8\,\mathrm{MHz}$ by applying a suitable off-axis magnetic field without changing the SiV level splitting, as we show in a detailed microscopic analysis in the supplemental material [38]. Using $g_\mathrm{sm}/2\pi = 2\,\mathrm{MHz}$ as a conservative estimate and assuming a detuning $\Delta_\mathrm{sm} \equiv \omega_\mathrm{m} - \omega_\mathrm{s} = 2\pi \times 150\,\mathrm{MHz}$, a dispersive coupling $\chi \equiv g_\mathrm{sm}^2/\Delta_\mathrm{sm} = 2\pi \times 27\,\mathrm{kHz}$ appears to be realistic. The corresponding ratio $\chi/\Gamma_\mathrm{mech} = 0.13$ is indicated by the gray vertical line in Fig. 2.

With these numbers, and using low probe-laser power [such that $n_\mathrm{mech}(\tau_\mathrm{meas})$ is more than an order of magnitude below $n_\mathrm{mech}^\mathrm{crit}$, see inset of Fig. 2], we find an estimated measurement time of $\tau_\mathrm{meas} = 3.31\,\mu\mathrm{s}$. This could be further decreased by using a stronger probe laser. Our τ_meas is thus competitive with optical readout times of $13\,\mu\mathrm{s}$ for highly strained SiV centers in a diamond nanocavity [39] and $30\,\mu\mathrm{s}$ for optical fluorescence readout of SiV centers with an external magnetic field precisely aligned along the SiV axis. In the latter case, the measurement times were limited by the repolarization of the SiV into its ground state on a timescale $\approx 30\,\mathrm{ms}$. For OMIT readout, the estimated measurement times are an order of magnitude shorter, and they will be limited by a Purcell decay time of $\tau_\mathrm{Purcell} \approx 28\,\mathrm{ms}$ [38]. We thus find $\tau_\mathrm{Purcell}/\tau_\mathrm{meas} \approx 8500 \ggg 1$, which could be further increased by increasing Δ_sm [48].

Application for quantum sensing— Our OMIT measurement scheme can also be used for more general parameter estimation where the goal is to detect an unknown signal that causes a small mechanical frequency shift $\varepsilon \ll \omega_\mathrm{m}$. This basic sensing scheme is widely used, e.g., in atomic-force microscopy (AFM) [41, 42] and mass sensing [43], and it has also been suggested for new OM sensing protocols using limit cycles [49]. Here, with quantum sensing in mind, we are interested in the fundamental limits on the estimation error of such schemes. OMIT allows one to improve the estimation error beyond that of standard schemes using continuous mechanical position detection. Such schemes are fundamentally limited by the standard quantum limit of position detection (SQL-PD) [50, 51]. The estimation error for infinitesimal frequency changes is $(\mathbf{\Delta}\varepsilon)^2(\tau) = \lim_{\varepsilon \to 0} \langle [\widehat{\delta\mathcal{I}}(\tau)]^2 \rangle_\varepsilon / |\partial_\varepsilon \langle \hat{\mathcal{I}}(\tau) \rangle_\varepsilon|^2$, which is optimized for a
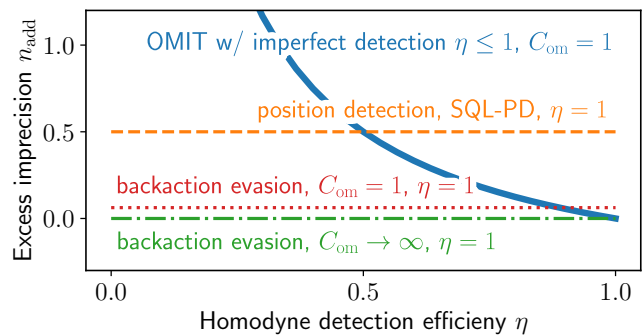

FIG. 3. Comparison of the excess imprecision noise n_add [expressed in terms of an equivalent amount of thermal phonons, see Eq. (7)], for sensing a small mechanical frequency shift $\varepsilon \ll \omega_\mathrm{m}$ with different measurement schemes. The thick blue line indicates an OMIT measurement with imperfect homodyne detection (efficiency $0 \leq \eta \leq 1$). The thin horizontal lines indicate the smallest excess imprecision noise achievable with other schemes in the limit of perfect homodyne detection, $\eta = 1$.

resonant probe laser and $C_\mathrm{om} = 1$ [38],

$$(\mathbf{\Delta}\varepsilon)^2(\tau) = \frac{\Gamma_\mathrm{mech}}{4 n_\mathrm{mech}^\mathrm{ss} \tau}(1 + 2n_\mathrm{th} + 2n_\mathrm{add})\,. \tag{7}$$

Here, n_th denotes the thermal phonon number due to interaction of the mechanical mode with a finite-temperature environment, and n_add represents potential imprecision noise due to the readout of the mechanics, expressed in terms of an equivalent amount of thermal phonons. Note that AFM and limit-cycle sensing protocols yield the same estimation error (7) but are limited by thermal noise, $n_\mathrm{th} \gg 1$ and thus typically not sensitive to fundamental imprecision noise [42, 49]. Also note that our goal is not to change the fundamental scaling with $n_\mathrm{mech}^\mathrm{ss}$, but to make n_add as small as possible.

In the ideal case analyzed so far, we have $n_\mathrm{add} = 0$ for OMIT readout even when all quantum effects are included. To highlight the significance of this result, it is instructive to compare Eq. (7) with other measurement schemes to determine a small frequency shift ε. Perhaps the most obvious approach is to drive the mechanical resonator linearly at ω_m and continuously measure its position $\hat{x} = x_\mathrm{zpf}(\hat{b} + \hat{b}^\dagger)$, where x_zpf denotes the zero-point fluctuations. This signal can then be used to determine the phase lag between $\langle \hat{x}(t) \rangle$ and the drive (and hence ε). Since this measurement collects information on both quadratures of $\hat{x}(t)$, its estimation error can at best reach the SQL-PD with $n_\mathrm{add} = 1/2$ [50, 51].

The SQL-PD can be surpassed by performing a backaction-evading (BAE) measurement [52, 53], which is tuned to measure only the phase quadrature of $\hat{x}(t)$ containing information on ε. In the limit of a large cooperativity $C_\mathrm{om} \to \infty$, one finds $n_\mathrm{add} \to 0$ and thus achieves *the same estimation error* as our OMIT scheme. While

BAE measurements (which necessarily require large C_{om}) have been demonstrated [54–58], they are experimentally far more challenging than a simple OMIT measurement with $C_{om} = 1$ (something that is routinely done for characterization purposes).

Note that both direct position detection and BAE measurements require careful phase tuning between the mechanical drive and the local oscillator of the homodyne detection. In contrast, our OMIT scheme is an all-optical measurement where the optical probe tone (driving the mechanics) and the local oscillator can be derived from the same laser, eliminating the need for a separate mechanical drive and its phase control.

The absence of added noise in the OMIT scheme is due to the fact that OMIT (unlike position detection and BAE measurements) transduces both mechanical quadratures into quadratures of the optical output field *without any gain* [38]. By adjusting the local-oscillator phase, one can then choose to measure the optical quadrature $\propto \varepsilon$. Amplification of mechanical quadratures is not required since once can increase the signal by driving the mechanics more strongly, which gives rise to the $1/n_{mech}^{ss}$ scaling in Eq. (7). In Fig. 3, we also analyze the case of imperfect homodyne detection (efficiency $0 \leq \eta \leq 1$). In this case, there will be added noise $n_{add} = (1 - \eta)/2\eta$, but state-of-the-art OMIT detection will surpass the SQL-PD for experimentally feasible efficiencies $\eta \gtrsim 70\%$ [59].

Conclusion— Our work presents a potentially powerful alternative readout scheme for solid-state spin defects with large strain coupling. This coupling allows one to perform dispersive spin readout using a mechanical mode, which is optically driven and read out using an OMIT scheme [60]. For SiV defects in a diamond OMCs, the estimated readout times are an order of magnitude shorter than the best measurement times for single-shot optical fluorescence readout. Besides spin readout, our scheme is also useful for quantum sensing, when a small signal modifies the resonance frequency of a mechanical oscillator, e.g., strain-mediated readout of the collective state of a large ensemble of NV centers. It would be interesting to check if OMIT readout can also be applied to other types of solid-state spin defects with strain coupling.

Our protocol could be combined with existing ideas to generate remote entanglement between two distant superconducting qubits using dispersive measurements [61, 62], requiring only small modifications of recent experiments coupling superconducting qubits to mechanical modes [63–66].

---

[1] V. M. Acosta, E. Bauch, M. P. Ledbetter, C. Santori, K. M. C. Fu, P. E. Barclay, R. G. Beausoleil, H. Linget, J. F. Roch, F. Treussart, S. Chemerisov, W. Gawlik, and D. Budker, Phys. Rev. B **80**, 115202 (2009).

[2] S. Steinert, F. Dolde, P. Neumann, A. Aird, B. Naydenov, G. Balasubramanian, F. Jelezko, and J. Wrachtrup, Review of Scientific Instruments **81**, 043705 (2010).

[3] L. M. Pham, D. L. Sage, P. L. Stanwix, T. K. Yeung, D. Glenn, A. Trifonov, P. Cappellaro, P. R. Hemmer, M. D. Lukin, H. Park, A. Yacoby, and R. L. Walsworth, New Journal of Physics **13**, 045021 (2011).

[4] T. Wolf, P. Neumann, K. Nakamura, H. Sumiya, T. Ohshima, J. Isoya, and J. Wrachtrup, Phys. Rev. X **5**, 041001 (2015).

[5] D. D. Awschalom, R. Hanson, J. Wrachtrup, and B. B. Zhou, Nature Photonics **12**, 516 (2018).

[6] H. J. Mamin, M. Kim, M. H. Sherwood, C. T. Rettner, K. Ohno, D. D. Awschalom, and D. Rugar, Science **339**, 557 (2013).

[7] T. Staudacher, F. Shi, S. Pezzagna, J. Meijer, J. Du, C. A. Meriles, F. Reinhard, and J. Wrachtrup, Science **339**, 561 (2013).

[8] J. M. Taylor, P. Cappellaro, L. Childress, L. Jiang, D. Budker, P. R. Hemmer, A. Yacoby, R. Walsworth, and M. D. Lukin, Nature Physics **4**, 810 (2008).

[9] L. Rondin, J.-P. Tetienne, T. Hingant, J.-F. Roch, P. Maletinsky, and V. Jacques, Reports on Progress in Physics **77**, 056503 (2014).

[10] F. Dolde, H. Fedder, M. W. Doherty, T. Nöbauer, F. Rempp, G. Balasubramanian, T. Wolf, F. Reinhard, L. C. L. Hollenberg, F. Jelezko, and J. Wrachtrup, Nature Physics **7**, 459 (2011).

[11] V. M. Acosta, E. Bauch, M. P. Ledbetter, A. Waxman, L.-S. Bouchard, and D. Budker, Phys. Rev. Lett. **104**, 070801 (2010).

[12] V. Giovannetti, S. Lloyd, and L. Maccone, Science **306**, 1330 (2004).

[13] C. L. Degen, F. Reinhard, and P. Cappellaro, Rev. Mod. Phys. **89**, 035002 (2017).

[14] L. Pezzè, A. Smerzi, M. K. Oberthaler, R. Schmied, and P. Treutlein, Rev. Mod. Phys. **90**, 035005 (2018).

[15] J. F. Barry, J. M. Schloss, E. Bauch, M. J. Turner, C. A. Hart, L. M. Pham, and R. L. Walsworth, Rev. Mod. Phys. **92**, 015004 (2020).

[16] S. Meesala, Y.-I. Sohn, H. A. Atikian, S. Kim, M. J. Burek, J. T. Choy, and M. Lončar, Phys. Rev. Applied **5**, 034010 (2016).

[17] D. Lee, K. W. Lee, J. V. Cady, P. Ovartchaiyapong, and A. C. B. Jayich, Journal of Optics **19**, 033001 (2017).

[18] S. Meesala, Y.-I. Sohn, B. Pingault, L. Shao, H. A. Atikian, J. Holzgrafe, M. Gündogan, C. Stavrakas, A. Sipahigil, C. Chia, R. Evans, M. J. Burek, M. Zhang, L. Wu, J. L. Pacheco, J. Abraham, E. Bielejec, M. D. Lukin, M. Atatüre, and M. Lončar, Phys. Rev. B **97**, 205444 (2018).

[19] K. V. Kepesidis, M.-A. Lemonde, A. Norambuena, J. R.

Maze, and P. Rabl, Phys. Rev. B **94**, 214115 (2016).

[20] E. R. MacQuarrie, T. A. Gosavi, N. R. Jungwirth, S. A. Bhave, and G. D. Fuchs, Phys. Rev. Lett. **111**, 227602 (2013).

[21] E. R. MacQuarrie, T. A. Gosavi, A. M. Moehle, N. R. Jungwirth, S. A. Bhave, and G. D. Fuchs, Optica **2**, 233 (2015).

[22] A. Barfuss, J. Teissier, E. Neu, A. Nunnenkamp, and P. Maletinsky, Nature Physics **11**, 820 (2015).

[23] K. W. Lee, D. Lee, P. Ovartchaiyapong, J. Minguzzi, J. R. Maze, and A. C. Bleszynski Jayich, Phys. Rev. Applied **6**, 034005 (2016).

[24] D. A. Golter, T. Oo, M. Amezcua, K. A. Stewart, and H. Wang, Phys. Rev. Lett. **116**, 143602 (2016).

[25] P. Groszkowski, M. Koppenhöfer, H.-K. Lau, and A. A. Clerk, Phys. Rev. X **12**, 011015 (2022).

[26] J. M. Kitzman, J. R. Lane, C. Undershute, P. M. Harrington, N. R. Beysengulov, C. A. Mikolas, K. W. Murch, and J. Pollanen, arXiv , 2208.07423v1 (2022).

[27] M. Eichenfield, J. Chan, R. M. Camacho, K. J. Vahala, and O. Painter, Nature **462**, 78 (2009).

[28] M. J. Burek, J. D. Cohen, S. M. Meenehan, N. El-Sawah, C. Chia, T. Ruelle, S. Meesala, J. Rochman, H. A. Atikian, M. Markham, D. J. Twitchen, M. D. Lukin, O. Painter, and M. Lončar, Optica **3**, 1404 (2016).

[29] J. V. Cady, O. Michel, K. W. Lee, R. N. Patel, C. J. Sarabalis, A. H. Safavi-Naeini, and A. C. B. Jayich, Quantum Science and Technology **4**, 024009 (2019).

[30] A. Blais, A. L. Grimsmo, S. M. Girvin, and A. Wallraff, Rev. Mod. Phys. **93**, 025005 (2021).

[31] A. Schliesser, *Cavity optomechanics and optical frequency comb generation with silica whispering-gallery-mode resonators*, Ph.D. thesis, Ludwig-Maximilians-Universität München (2009).

[32] G. S. Agarwal and S. Huang, Phys. Rev. A **81**, 041803(R) (2010).

[33] S. Weis, R. Rivière, S. Deléglise, E. Gavartin, O. Arcizet, A. Schliesser, and T. J. Kippenberg, Science **330**, 1520 (2010).

[34] A. H. Safavi-Naeini, T. P. M. Alegre, J. Chan, M. Eichenfield, M. Winger, Q. Lin, J. T. Hill, D. E. Chang, and O. Painter, Nature **472**, 69 (2011).

[35] R. D. Delaney, M. D. Urmey, S. Mittal, B. M. Brubaker, J. M. Kindem, P. S. Burns, C. A. Regal, and K. W. Lehnert, Nature **606**, 489 (2022).

[36] While there are many differences [38], the most crucial is that our scheme has fewer basic ingredients: there is no microwave resonator or drive, nor any microwave-optomechanical coupling.

[37] P. K. Shandilya, D. P. Lake, M. J. Mitchell, D. D. Sukachev, and P. E. Barclay, Nature Physics **17**, 1420 (2021).

[38] See Supplemental Material at [URL will be inserted by publisher] for additional details on the OMIT readout protocol, which includes Refs. [67–88].

[39] C. T. Nguyen, D. D. Sukachev, M. K. Bhaskar, B. Machielse, D. S. Levonian, E. N. Knall, P. Stroganov, R. Riedinger, H. Park, M. Lončar, and M. D. Lukin, Phys. Rev. Lett. **123**, 183602 (2019).

[40] D. D. Sukachev, A. Sipahigil, C. T. Nguyen, M. K. Bhaskar, R. E. Evans, F. Jelezko, and M. D. Lukin, Phys. Rev. Lett. **119**, 223602 (2017).

[41] Y. Martin, C. C. Williams, and H. K. Wickramasinghe, Journal of Applied Physics **61**, 4723 (1987).

[42] T. R. Albrecht, P. Grütter, D. Horne, and D. Rugar, Journal of Applied Physics **69**, 668 (1991).

[43] K. L. Ekinci, Y. T. Yang, and M. L. Roukes, Journal of Applied Physics **95**, 2682 (2004).

[44] See [38] for the case of nonzero mechanical temperature.

[45] M. Aspelmeyer, T. J. Kippenberg, and F. Marquardt, Rev. Mod. Phys. **86**, 1391 (2014).

[46] N. Didier, A. Kamal, W. D. Oliver, A. Blais, and A. A. Clerk, Phys. Rev. Lett. **115**, 093604 (2015).

[47] Here, we always choose the optical probe power small enough to keep $n_{\mathrm{mech}}^{\mathrm{ss}}$ below the critical phonon number. Thanks to the extreme linearity of mechanical modes in OMCs and the small bare optomechanical coupling strength, $n_{\mathrm{mech}}^{\mathrm{ss}} \gg 1$ does not lead to a breakdown of the linearized optomechanical Hamiltonian.

[48] Given such a large value of $\chi/\Gamma_{\mathrm{mech}}$, one may worry that the spin-mechanical coupling degrades the coherence properties of the SiVs. However, resonant interactions with phonon modes other than the mechanical mode of interest can be suppressed by a suitable design of the OMC. Dephasing of the SiV is irrelevant for spin readout but it may still limit the operation of the SiV as a quantum sensor. Yet, the main phonon-induced dephasing mechanism is dispersive coupling to off-resonant several-GHz phonon modes, which will be highly suppressed at temperatures below $100\,\mathrm{mK}$ [38].

[49] B. Guha, P. E. Allain, A. Lemaître, G. Leo, and I. Favero, Phys. Rev. Applied **14**, 024079 (2020).

[50] V. B. Braginsky and F. Y. Khalili, *Quantum measurement*, edited by K. S. Thorne (Cambridge University Press, 1992).

[51] A. A. Clerk, M. H. Devoret, S. M. Girvin, F. Marquardt, and R. J. Schoelkopf, Rev. Mod. Phys. **82**, 1155 (2010).

[52] V. B. Braginsky, Y. I. Vorontsov, and K. S. Thorne, Science **209**, 547 (1980).

[53] A. A. Clerk, F. Marquardt, and K. Jacobs, New Journal of Physics **10**, 095010 (2008).

[54] J. B. Hertzberg, T. Rocheleau, T. Ndukum, M. Savva, A. A. Clerk, and K. C. Schwab, Nature Physics **6**, 213 (2010).

[55] J. Suh, A. J. Weinstein, C. U. Lei, E. E. Wollman, S. K. Steinke, P. Meystre, A. A. Clerk, and K. C. Schwab, Science **344**, 1262 (2014).

[56] F. Lecocq, J. B. Clark, R. W. Simmonds, J. Aumentado, and J. D. Teufel, Phys. Rev. X **5**, 041037 (2015).

[57] C. F. Ockeloen-Korppi, E. Damskägg, J.-M. Pirkkalainen, A. A. Clerk, M. J. Woolley, and M. A. Sillanpää, Phys. Rev. Lett. **117**, 140401 (2016).

[58] I. Shomroni, L. Qiu, D. Malz, A. Nunnenkamp, and T. J. Kippenberg, Nature Communications **10**, 2086 (2019).

[59] T. P. Purdy, P.-L. Yu, R. W. Peterson, N. S. Kampel, and C. A. Regal, Phys. Rev. X **3**, 031012 (2013).

[60] As an aside, the closely related phenomenon of optomechanically-induced amplification [34, 89, 90] could also be used for a similar readout scheme when additional signal amplification is needed, e.g., to overcome noise in the post-amplification stage.

[61] N. Roch, M. E. Schwartz, F. Motzoi, C. Macklin, R. Vijay, A. W. Eddins, A. N. Korotkov, K. B. Whaley, M. Sarovar, and I. Siddiqi, Phys. Rev. Lett. **112**, 170501 (2014).

[62] M. Silveri, E. Zalys-Geller, M. Hatridge, Z. Leghtas, M. H. Devoret, and S. M. Girvin, Phys. Rev. A **93**, 062310 (2016).

[63] U. von Lüpke, Y. Yang, M. Bild, L. Michaud, M. Fadel, and Y. Chu, Nature Physics **18**, 794 (2022).

[64] E. A. Wollack, A. Y. Cleland, R. G. Gruenke, Z. Wang, P. Arrangoiz-Arriola, and A. H. Safavi-Naeini, Nature **604**, 463 (2022).

[65] M. Mirhosseini, A. Sipahigil, M. Kalaee, and O. Painter, Nature **588**, 599 (2020).

[66] Specifically, in Refs. 63 and 64, strong dispersive coupling between a superconducting qubit and mechanical modes has been used for qubit-based readout of the mechanical state, but the mechanical mode was not yet part of an optomechanical system. In addition, conversion of the excitation of a superconducting qubit into an optical photon using piezoelectric coupling to an OMC has been demonstrated in Ref. 65, but the qubit-mechanical interaction was resonant and only a single red-detuned optical drive had been applied.

[67] M. Aspelmeyer, T. J. Kippenberg, and F. Marquardt, eds., *Cavity Optomechanics* (Springer Berlin, Heidelberg, 2014).

[68] M.-A. Lemonde, N. Didier, and A. A. Clerk, Phys. Rev. Lett. **111**, 053602 (2013).

[69] A. Gali and J. R. Maze, Phys. Rev. B **88**, 235205 (2013).

[70] C. Hepp, *Electronic structure of the silicon vacancy color center in diamond*, Ph.D. thesis, Universität des Saarlandes (2014).

[71] C. Hepp, T. Müller, V. Waselowski, J. N. Becker, B. Pingault, H. Sternschulte, D. Steinmüller-Nethl, A. Gali, J. R. Maze, M. Atatüre, and C. Becher, Phys. Rev. Lett. **112**, 036405 (2014).

[72] B. Pingault, D.-D. Jarausch, C. Hepp, L. Klintberg, J. N. Becker, M. Markham, C. Becher, and M. AtatŒre, Nature Communications **8**, 15579 (2017).

[73] C. Chia, K. Kuruma, B. Pingault, and M. Lončar, in *2021 Conference on Lasers and Electro-Optics (CLEO)* (2021) pp. 1–2.

[74] R. Debroux, C. P. Michaels, C. M. Purser, N. Wan, M. E. Trusheim, J. Arjona Martínez, R. A. Parker, A. M. Stramma, K. C. Chen, L. de Santis, E. M. Alexeev, A. C. Ferrari, D. Englund, D. A. Gangloff, and M. Atatüre, Phys. Rev. X **11**, 041041 (2021).

[75] B. C. Rose, D. Huang, Z.-H. Zhang, P. Stevenson, A. M. Tyryshkin, S. Sangtawesin, S. Srinivasan, L. Loudin, M. L. Markham, A. M. Edmonds, D. J. Twitchen, S. A. Lyon, and N. P. de Leon, Science **361**, 60 (2018).

[76] B. L. Green, M. W. Doherty, E. Nako, N. B. Manson, U. F. S. D'Haenens-Johansson, S. D. Williams, D. J. Twitchen, and M. E. Newton, Phys. Rev. B **99**, 161112(R) (2019).

[77] Z.-H. Zhang, P. Stevenson, G. m. H. Thiering, B. C. Rose, D. Huang, A. M. Edmonds, M. L. Markham, S. A. Lyon, A. Gali, and N. P. de Leon, Phys. Rev. Lett. **125**, 237402 (2020).

[78] J. R. Maze, A. Gali, E. Togan, Y. Chu, A. Trifonov, E. Kaxiras, and M. D. Lukin, New Journal of Physics **13**, 025025 (2011).

[79] P. Ovartchaiyapong, K. W. Lee, B. A. Myers, and A. C. B. Jayich, Nature Communications **5**, 4429 (2014).

[80] J. Teissier, A. Barfuss, P. Appel, E. Neu, and P. Maletinsky, Phys. Rev. Lett. **113**, 020503 (2014).

[81] H. Seo, A. L. Falk, P. V. Klimov, K. C. Miao, G. Galli, and D. D. Awschalom, Nature Communications **7**, 12935 (2016).

[82] D. J. Christle, P. V. Klimov, C. F. De las Casas, K. Szász, V. Ivády, V. Jokubavicius, J. Ul Hassan, M. Syväjärvi, W. F. Koehl, T. Ohshima, N. T. Son, E. Janzén, A. Gali, and D. D. Awschalom, Phys. Rev. X **7**, 021046 (2017).

[83] A. L. Falk, P. V. Klimov, B. B. Buckley, V. Ivády, I. A. Abrikosov, G. Calusine, W. F. Koehl, A. Gali, and D. D. Awschalom, Phys. Rev. Lett. **112**, 187601 (2014).

[84] X. Lu, J. Y. Lee, and Q. Lin, Scientific Reports **5**, 17005 (2015).

[85] X. Lu, J. Y. Lee, and Q. Lin, Applied Physics Letters **116**, 221104 (2020).

[86] O. O. Soykal and T. L. Reinecke, Phys. Rev. B **95**, 081405(R) (2017).

[87] G. C. Vásquez, M. E. Bathen, A. Galeckas, C. Bazioti, K. M. Johansen, D. Maestre, A. Cremades, Ø. Prytz, A. M. Moe, A. Y. Kuznetsov, and L. Vines, Nano Letters **20**, 8689 (2020).

[88] C. M. Caves, Phys. Rev. D **26**, 1817 (1982).

[89] F. Massel, T. T. Heikkilä, J.-M. Pirkkalainen, S. U. Cho, H. Saloniemi, P. J. Hakonen, and M. A. Sillanpää, Nature **480**, 351 (2011).

[90] F. Hocke, X. Zhou, A. Schliesser, T. J. Kippenberg, H. Huebl, and R. Gross, New Journal of Physics **14**, 123037 (2012).